

Vector Meson Photoproduction with Linearly Polarized Beam

V. Mathieu,^{1,*} A. P. Szczepaniak,^{1,2,3} G. Fox,⁴ and Others

(Joint Physics Analysis Center)

¹*Theory Center, Thomas Jefferson National Accelerator Facility, Newport News, VA 23606, USA*

²*Center for Exploration of Energy and Matter, Indiana University, Bloomington, IN 47403, USA*

³*Physics Department, Indiana University, Bloomington, IN 47405, USA*

⁴*School of Informatics, Computing, and Engineering,
Indiana University, Bloomington, IN 47405, USA*

We propose a model describing the photoproduction of light vector meson photoproduction. The model is optimized for the description the spin density matrix elements of ω , ρ^0 and ϕ photoproduction at $E_\gamma \sim 9$ GeV. Prediction are given for the future measurements by the GlueX collaboration.

* vmathieu@jlab.org

I. INTRODUCTION

With the advent of the 12 GeV era at the Jefferson Lab, there is a growing interest for the photoproduction of light mesons. GlueX, whose main goal is the identification of gluonic excitation [1], is currently taking data with linearly polarized beam. The GlueX physics program will be soon complemented with the CLAS12 program on meson spectroscopy [2] and its unpolarized virtual photon beam.

The first measurement performed by the GlueX collaboration concerned the beam asymmetry of neutral pion and eta meson photoproduction [3]. The new GlueX measurement indicates that production of these pseudoscalar at high energies is strongly dominated by vector exchanges, in contradiction with the original SLAC measurement [4]. The latter displayed significant axial-vector contributions. Moreover the energy independence of these axial-vector contribution measured at SLAC was clearly in contradiction with the natural expectation in Regge theory [5]. GlueX, having their polarized data at a fixed energy, cannot test the energy dependence of the pseudoscalar beam asymmetry. Other similar measurements are therefore required to refine our understanding of the production mechanism of light meson photoproduction.

Light vector mesons, ρ , ω and ϕ , are copiously produced in the 4-12 GeV energy range. These vector mesons are not stable but are reconstructed from their decaying particles. Their narrow peaks are easily identified making the photoproduction of vector meson the natural reactions to test the reconstruction chain of new detectors. Moreover, assuming the dominance of a spin 1 resonance, one can relate the angular distribution of the daughters to the production mechanism of the resonance [6]. The spin density matrix elements (SDME) are the Rosetta stone relating experimental quantities, the angular distribution, to theoretical quantities, the helicity amplitudes. The first measurement of SDME for the photoproduction of vector meson was obtained at SLAC [7]. The implication of these data on helicity amplitudes were already discussed in the original publication [7]. Nevertheless the conclusions was rather quantitative. The lack of a model for the vector meson photoproduction prevented to draw quantitative conclusion. In this paper, we address this issue by presenting a simple model of vector meson photoproduction. Our model allows one to quantify the relative strength of various exchanges, and, for each exchange, to quantify their helicity couplings.

There are nine SDME accessible with a linearly polarized beam. They are functions of both the momentum transferred and the total energy. Describing nine functions of two variables is a challenging task and simplifications, depending on the kinematical region, are required. Above the resonance region, vector meson are produced via the exchange of Regge poles, whose energy dependence is known and factorizes out. The momentum transferred dependence of each contribution remains thus the only unknown.

Models in the literature [8–15] describe the production of vector meson in term of Regge exchanges with various momentum transferred dependence for each individual contribution. For most of them focuses only on the transferred momentum dependence of the differential cross section, described by form factors. In these models, the helicity structure of the photon-vector meson vertex is hidden behind effective interactions. However at high energy and in the nearly forward direction, the momentum transferred dependence can be inferred from the factorization and the conservation of angular momentum. The purpose of this paper is to provide a intuitive and flexible parametrization, encoding the kinematic dependences required by the Regge theory, for the description of the vector meson photoproduction SDME.

We will determine the momentum transferred of each relevant contribution from theoretical expectations and the data available. Our strategy is the following: We first list all exchanges in Section II. From the SLAC data we isolate the unnatural components of SDME for ρ^0 and ω production. Since, within uncertainties, these components are consistent with only spin-zero exchanges we will only consider π and η meson exchange and neglect other unnatural exchanges. Then we assume a factorized form for each natural contribution, Pomeron, f_2 and a_2 exchange. The momentum transferred dependence of each vertex is derived from the high energy limit. We relegate the extraction of the momentum transferred dependence in Appendix C. In Section III, we determined the parameters of our model. The normalization of the natural exchanges is extracted from total cross sections and the vector meson dominance assumption. Then their helicity couplings are fitted on the natural components of the SLAC data at 9.3 GeV. In Section IV, we compare the results our model to the world data and provide prediction for the future measurements of light vector mesons at GlueX. Finally our conclusion are presented in Section V. We recall the definitions of the common frames and the relation in Appendix A. For completeness, the relation between helicity amplitudes and SDME are indicated in Appendix B.

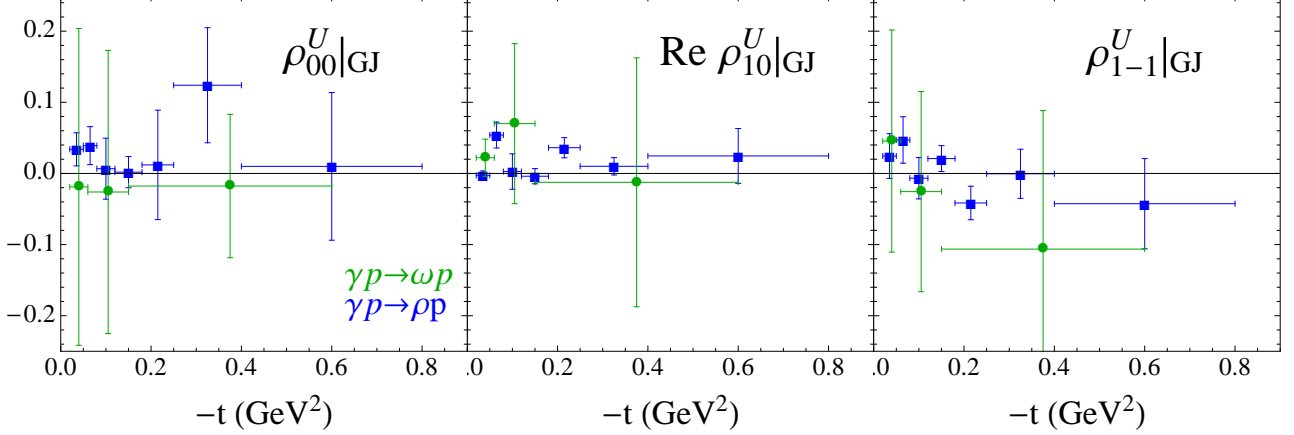


FIG. 1. Unnatural components of ω and ρ^0 spin density matrix elements at $E_\gamma = 9.3$ GeV. Data from Ref. [7].

II. EXCHANGES

At high energies, a vector meson is photoproduced diffractively via Pomeron exchange and Regge exchanges. The Regge exchanges have positive charge conjugation and non “exotic” quantum numbers (in the quark model sense).¹ Regge trajectories are classified according to their isospin I , parity P , charge conjugation C , G -parity $G = C(-1)^I$ and naturality $\eta = P(-1)^J$. The spin of the exchange J is not defined and as usual we will denote the Regge exchanges by their corresponding lowest spin meson:

$I^G J^{PC}$	$I^G J^{PC}$	$I^G J^{PC}$	
$a_2 : 1^- 2^{++}$	$\pi : 1^- 0^{-+}$	$a_1 : 1^- 1^{++}$	
$f_2 : 0^+ 2^{++}$	$\eta : 0^+ 0^{-+}$	$f_1 : 0^+ 1^{++}$	(1)

Among all unnatural exchanges,² the pion and the eta meson being closer to the scattering region, are expected to be the dominant one. We can check this assertion with the unnatural combination of SDME in the Gottfried-Jackson (GJ) frame on Fig. 1. As explained in App. A, the SDME in the GJ frame are equivalent to the SDME in the t -channel frame, the rest frame of the exchanges. The GJ frame thus allows us to probe the spin structure of the exchange. The elements ρ_{00}^U , $\text{Re } \rho_{010}^U$ and ρ_{1-1}^U are all consistent with zero in the whole t range and for both ω and ρ^0 photoproduction. The unnatural components of the SDME can be therefore described by solely spin-0 exchange.

At high energy, the amplitudes for a pion and a eta meson exchange reads

$$\mathcal{M}_{\lambda_V, \lambda_\gamma}^P(s, t) = \beta_0^P \lambda_\gamma \delta_{-\lambda, \lambda'} \sqrt{-t} \left[\delta_{\lambda_\gamma}^{\lambda_\omega} - \sqrt{2} \lambda_\gamma \frac{\sqrt{-t}}{m_V} \delta_0^{\lambda_\omega} + \frac{-t}{m_V^2} \delta_{-\lambda_\gamma}^{\lambda_\omega} \right] \frac{1 + e^{-i\pi\alpha_\pi(t)}}{2 \sin \alpha_\pi(t)} \left(\frac{s}{s_0} \right)^{\alpha_\pi(t)} \quad (2)$$

with $\beta_0^P = -m_V^2 \pi \alpha' (g_{V\gamma\pi} g_{\pi NN} + g_{V\gamma\eta} g_{\eta NN})/2$. The helicities are defined in the center-of-mass frame of the reaction $\gamma(k, \lambda_\gamma) N(p, \lambda) \rightarrow V(q, \lambda_V) N'(p', \lambda')$, also called the s -channel frame. We have considered the same Regge trajectory $\alpha_\pi(t)$ for the eta meson and the pion exchanges. This hypothesis yields a better comparison to the data in phi photoproduction as explained in Sec. IV. We refer to App. C for the derivation of the high energy limit of our exchange model amplitudes. However, it is worth describing the interpretation of each term in Eq. (C7).

According to Regge theory [16], the energy dependence factorizes into a power-law dependence $s^{\alpha_\pi(t)}$ and the phase is dictated by the factor $1 + e^{-i\pi\alpha_\pi(t)}$. This factor cancel the spin odd poles induced by the denominator $\sin \alpha_\pi(t)$. The factor λ_γ ensures that only real photons contribute and that the parity of the exchange is negative. The factor in the brackets involves all possible helicity structures at the photon-vector meson vertex. Each unit of helicity flip

¹ The trajectories having $PC = -+$ and $(-1)^J = -1$ does not coupled to two nucleons.

² Natural (unnatural) exchanges are trajectories involving positive (negative) naturality mesons.

costs a factor $\sqrt{-t}$ normalized by m_V , the only scale at this vertex. The helicity of the photon needs indeed to be conserved in the forward direction. As explained in App. C, this factors originate from the half-angle factor of the partial wave decomposition, *i.e.* $\sin \theta_s/2 \rightarrow \sqrt{-t'}/s$ with θ_s , the scattering angle in the s -channel frame. Thorough this paper, we will always neglect t_{\min} in $t' = t - t_{\min}$ as $t_{\min}/m_V^2 \rightarrow -(m_V/2p_{\text{lab}})^2$ is of order of 10^{-3} for $p_{\text{lab}} = 9$ GeV. Finally the factor $\delta_{-\lambda'}^\lambda \sqrt{-t}$ comes from the pion-nucleon vertex.

For the natural components of the SDME, we will consider the Pomeron, f_2 and a_2 exchanges. Although some models incorporated a scalar exchange, representing a 2 pion exchange, in omega photoproduction [15], this contribution is negligible at 9 GeV.

We will assume factorization into a top and a bottom vertex together with a Regge factor:

$$\mathcal{M}_{\lambda_V, \lambda_\gamma}^R(s, t) = \beta_R^{\gamma V} e^{b_R t} V_{\lambda_V \lambda_\gamma}^{\gamma V}(t) R(s, t) V_{\lambda' \lambda}^{pp}(t) \quad (3)$$

We have pulled out the normalization factor $\beta_R^{\gamma V}$ and the exponential fall-off, needed to reproduce the empirical shrinkage of the differential cross section. Our electromagnetic vertex involves the three general possible helicity structures: helicity non-flip, single-flip and double-flip. To each of these structure is associated a factor $\sqrt{-t}/m_V$ as explained above:

$$V_{\lambda_V \lambda_\gamma}^{\gamma V}(t) = \lambda_\gamma^2 \left(\delta_{\lambda_\gamma}^{\lambda_V} + \beta_1^R \frac{\sqrt{-t}}{m_V} \frac{\lambda_\gamma}{\sqrt{2}} \delta_0^{\lambda_V} + \beta_2^R \frac{-t}{m_V^2} \delta_{-\lambda_\gamma}^{\lambda_V} \right). \quad (4)$$

As explained in App. C, this kinematical factor arises from the conservation of angular momentum and the factorization of Regge residues. Our nucleon vertex involves similarly the two possible nucleon structures:

$$V_{\lambda' \lambda}^{pp}(t) = \delta_{\lambda'}^\lambda + 2\lambda \kappa_R \frac{\sqrt{-t}}{2m} \delta_{-\lambda'}^\lambda. \quad (5)$$

In this case the scale factor to compensate the kinematical factor $\sqrt{-t}$ is provided by the nucleon mass m . Finally the energy dependence and the Regge phase are introduced *via* the factor

$$R(s, t) = \frac{\alpha_R(t)}{\alpha_R(0)} \frac{1 + e^{-i\pi\alpha_R(t)}}{\sin \pi\alpha_R(t)} \left(\frac{s}{s_0} \right)^{\alpha_R(t)}. \quad (6)$$

The factor $\alpha_R(t)/\alpha_R(0)$ simply removes the unphysical pole at $\alpha(t) = 0$ that arises in the scattering region for the f_2 and a_2 exchanges. For consistency we also include this factor for the Pomeron exchange although it doesn't affect the results.

Collecting the pieces, our model for the s -channel amplitudes of vector meson photoproduction is

$$\mathcal{M}_{\lambda_V, \lambda_\gamma}^P(s, t) = \mathcal{M}_{\lambda_V, \lambda_\gamma}^P(s, t) + \mathcal{M}_{\lambda_V, \lambda_\gamma}^f(s, t) + \mathcal{M}_{\lambda_V, \lambda_\gamma}^{f_2}(s, t) + \mathcal{M}_{\lambda_V, \lambda_\gamma}^{a_2}(s, t). \quad (7)$$

III. PARAMETERS DETERMINATION

We now turn our attention to the determination of the parameters of the model. The scale factor is $s_0 = 1 \text{ GeV}^2$. The trajectories of each exchanges are known and we take

$$\alpha_\pi(t) = 0.7(t - m_\pi^2) \quad \alpha_{\mathbb{P}}(t) = 1.08 + 0.2t \quad \alpha_{f_2, a_2}(t) = 0.5 + 0.9t. \quad (8)$$

The pion exchange piece involves known couplings. For the pion-nucleon and eta-nucleon couplings, we take $g_{\pi NN}^2/4\pi = 14$ and $g_{\eta NN}^2/4\pi = 2$. Our normalization for the electromagnetic vertex, cf. App. C, allow us to relate the couplings $g_{VP\gamma}$ to the decay widths $\Gamma(V \rightarrow \gamma P)$ in Eq. (C4). The relevant couplings are summarized in the Table I.

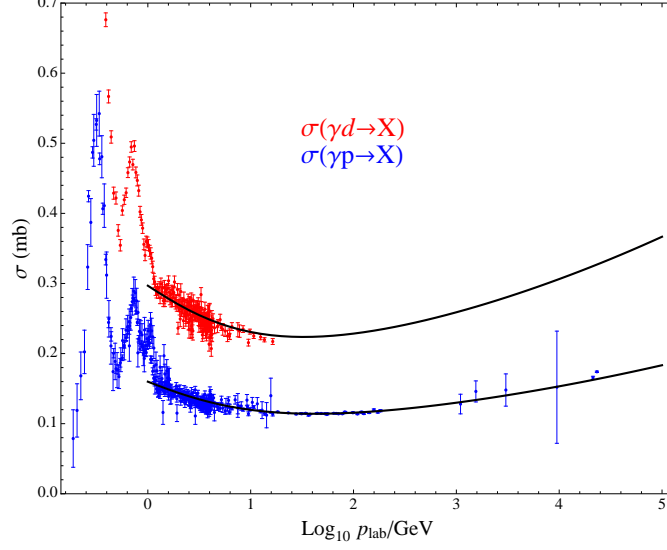
For each natural exchanges R we need to determine five parameters: $\beta_R^{\gamma V}, \beta_1^R, \beta_2^R, \kappa_R$ and b_R . The overall normalization $\beta_R^{\gamma V}$ of each of these exchanges can be obtained from the total γp and γd cross sections and vector meson dominances [17]. We fit the the data from the Review of Particle Physics [18] with the forms

$$\sigma(\gamma p) = \frac{389 \mu\text{b}}{2mp_{\text{lab}}} \left(\beta_{\mathbb{P}}^{\gamma\gamma} s^{1.08} + \left(\beta_{f_2}^{\gamma\gamma} + \beta_{a_2}^{\gamma\gamma} \right) s^{0.5} \right), \quad (9a)$$

$$\sigma(\gamma d) = \frac{389 \mu\text{b}}{2mp_{\text{lab}}} \left(2\beta_{\mathbb{P}}^{\gamma\gamma} s^{1.08} + 2\beta_{f_2}^{\gamma\gamma} s^{0.5} \right). \quad (9b)$$

TABLE I. Vector meson radiative width and pseudoscalar exchange couplings.

V	$\Gamma(V \rightarrow \gamma\pi^0)$	$g_{V\pi\gamma}$	$\Gamma(V \rightarrow \gamma\eta)$	$g_{V\eta\gamma}$
ω	703 KeV	0.696 GeV^{-1}	44.8 KeV	0.479 GeV^{-1}
ρ^0	89.6 KeV	0.252 GeV^{-1}	3.91 KeV	0.136 GeV^{-1}
ϕ	5.41 KeV	0.040 GeV^{-1}	56.8 KeV	0.210 GeV^{-1}

FIG. 2. Total cross section $\gamma p \rightarrow X$ (blue) and $\gamma d \rightarrow X$ (red). The black lines are the results of our fit. The data are taken from Ref. [18].

The comparison with the data is shown on Fig. 2.

In order to use vector meson dominance we use the following interaction between photon and vector meson, with J^μ the electromagnetic current:

$$\mathcal{L} = -eJ^\mu \left(\frac{m_\rho^2}{\gamma_\rho} \rho_\mu + \frac{m_\omega^2}{\gamma_\omega} \omega_\mu + \frac{m_\phi^2}{\gamma_\phi} \phi_\mu \right) \quad (10)$$

From this interaction and neglecting the electron mass, one gets the leptonic width $\Gamma(V \rightarrow e^+e^-) = m_V(\alpha^2/3)(4\pi/\gamma_V^2)$ which determines the couplings γ_V . They are indicated in Table II (we used $\alpha = e^2/4\pi = 1/137$). The SU(3) quark

TABLE II. Vector meson dominance parameters.

V	$\Gamma(V \rightarrow e^+e^-)$	$4\pi/\gamma_V^2$
ρ^0	7.04(6) keV	0.506(4)
ω	0.60(2) keV	0.044(1)
ϕ	1.26(1) keV	0.070(1)

model predictions $\gamma_\omega/\gamma_\rho = 3$ and $\gamma_\omega/\gamma_\phi = \sqrt{2}$ are approximatively satisfied by the vector meson couplings, *i.e.* $\gamma_\omega/\gamma_\rho = 3.4(6)$ and $\gamma_\omega/\gamma_\phi = 1.3(1)$. However, it is well-known that the ϕ meson differential cross section led to an effective value of γ_ϕ twice bigger than the one obtain from leptonic width [7]. For consistency, we will use the γ_ϕ value obtained from the leptonic width but we keep in mind this issue where comparing to the data.

We next assume that the Pomeron couples equally every light quarks [19] to extract the couplings at the photon-vector meson vertex:

$$\beta_{\mathbb{P}}^{\gamma V} = \beta_{\mathbb{P}}^{\gamma\gamma} \frac{e}{\gamma_V} \times \left(\frac{e^2}{\gamma_\rho^2} + \frac{e^2}{\gamma_\omega^2} + \frac{e^2}{\gamma_\phi^2} \right)^{-1} \quad (11a)$$

We note that by using a twice bigger value of γ_ϕ , the ω and ρ^0 couplings of the Pomeron would change by only 10%. For the Regge exchanges, we assume ideal mixing, *i.e.* $\beta_{f_2}^{\gamma\phi} = \beta_{a_2}^{\gamma\phi} = 0$ and extract the remaining couplings using again vector meson dominance:

$$\beta_{f_2}^{\gamma\omega,\rho} = \beta_{f_2}^{\gamma\gamma} \frac{e}{\gamma_{\omega,\rho}} \times \left(\frac{e^2}{\gamma_\rho^2} + \frac{e^2}{\gamma_\omega^2} \right)^{-1}, \quad (11b)$$

$$\beta_{a_2}^{\gamma\omega,\rho} = \beta_{f_2}^{\gamma\gamma} \frac{\gamma_{\omega,\rho}}{2e} \quad (11c)$$

In the first determination of the magnitude of the vector meson photoproduction differential cross section in the forward direction [19], Donnachie and Landshoff implicitly assumed the quark counting rule for the Regge exchanges f_2 and a_2 . They have scaled the Regge contribution by the same factor as for the Pomeron. The correct prediction for the Regge exchanges couplings from VMD is given by Eqs (11).

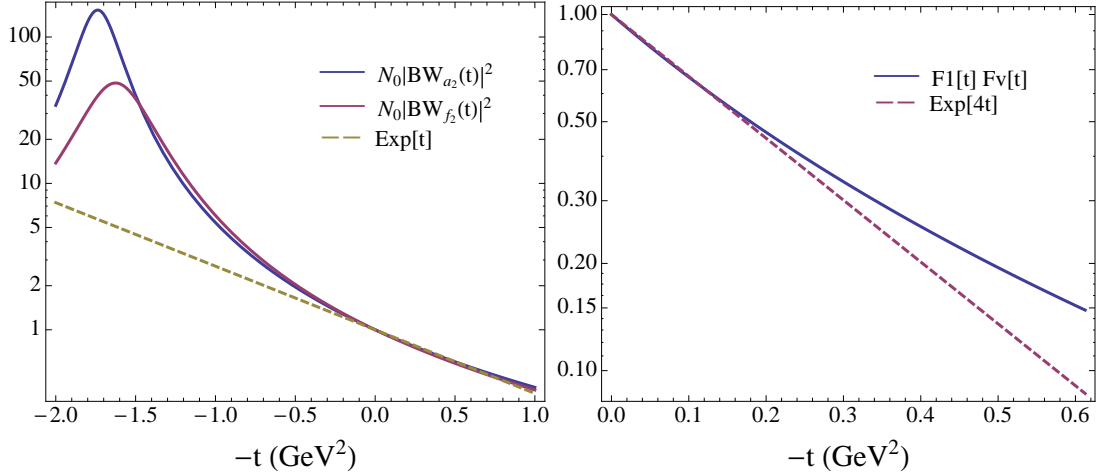


FIG. 3. Natural components of ω and ρ^0 photoproduction spin density matrix elements at $E_\gamma = 2.8, 4.7, 9.3$ GeV. Data from Ref. [7]. The lines are our model, determined on the 9.3 GeV data only.

For the exponential falloffs b_R we first consider the Pomeron form factor $F_1(t)F_V(t)$, used in Ref [20]

$$F_1(t) = \frac{4m^2 - 2.8t}{(4m^2 - t)(1 - t/t_0)^2}, \quad (12a)$$

$$F_V(t) = \frac{1}{1 - t/m_V^2} \frac{2\mu_0^2 + m_V^2}{2\mu_0^2 + m_V^2 - t}, \quad (12b)$$

with $\mu_0^2 = 1.1$ GeV², $t_0 = 0.7$ GeV². $F_1(t)$ is the dipole approximation of the nucleon Diract form factor [?] and F_V is an empirical form factor at the photon-vector meson vertex.³ For the f_2 and a_2 exchanges, we consider a Breit-Wigner parametrization of the tensor exchange,

$$BW(t) = \frac{m_R \Gamma_R}{m_R^2 - t - im_R \Gamma_R}. \quad (13)$$

Then we simply approximate these form factors by a exponential falloff. We obtain

$$|F_1(t)F_V(t)|^2 \sim e^{8t} \quad (14a)$$

$$|BW(t)|^2 \sim |BW(0)|^2 e^t. \quad (14b)$$

The comparison is presented on Fig. 3. We then use $b_{\mathbb{P}} = 4$ and $b_{f_2} = b_{a_2} = 0.5$.

³ We have renormalized it such that $F_V(0) = 1$.

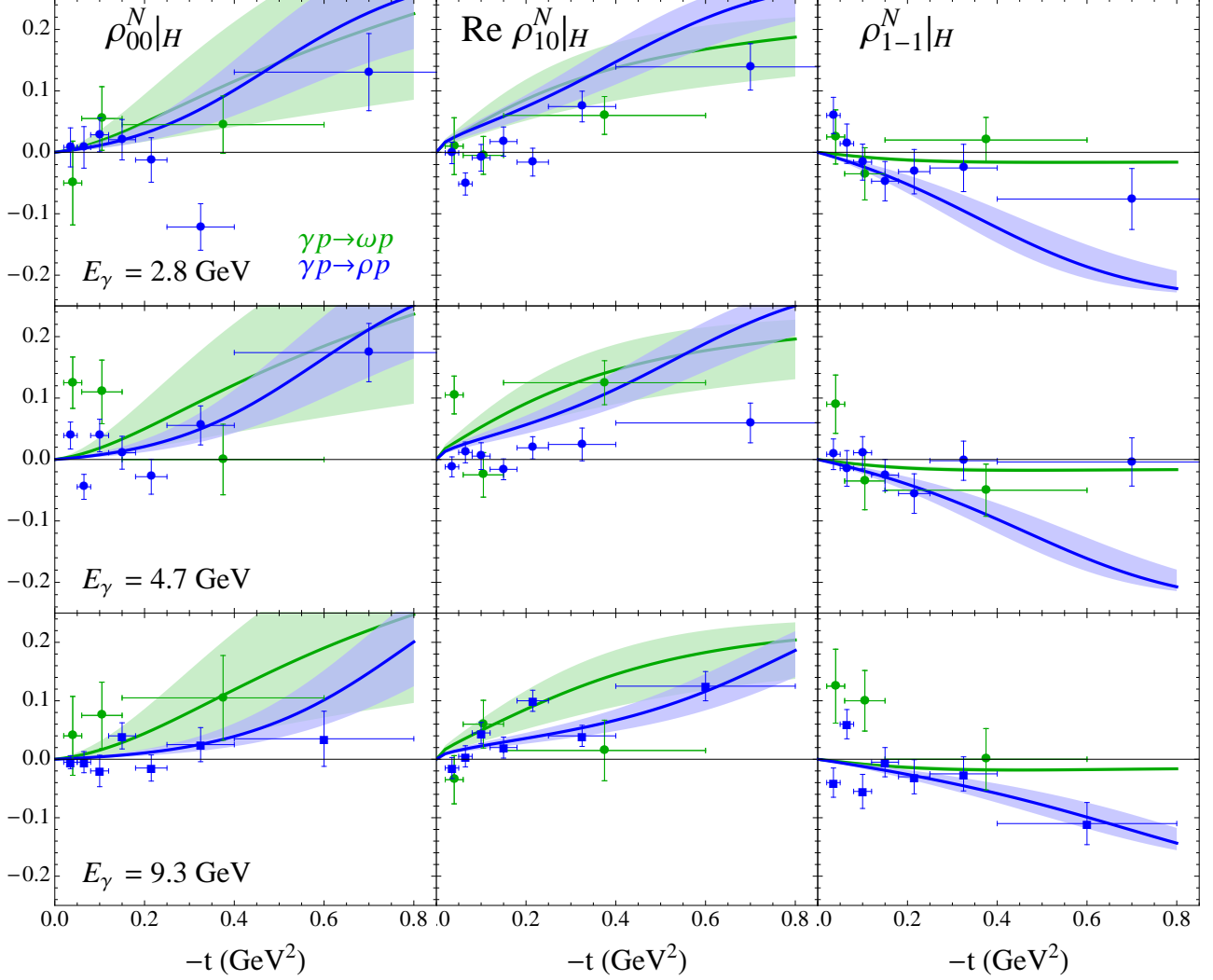


FIG. 4. Natural components of ω and ρ^0 photoproduction spin density matrix elements at $E_\gamma = 2.8, 4.7, 9.3$ GeV. Data from Ref. [7]. The lines are our model, determined on the 9.3 GeV data only.

Isoscalar exchange, f_2 and Pomeron, are empirically helicity non-flip at the nucleon vertex [21]. Accordingly we set $\kappa_{\mathbb{P}} = \kappa_{f_2} = 0$. The isovector have a stronger helicity flip component. We have set $\kappa_{a_2} = 8$ according to Ref. [21].

Finally to determine the helicity flip couplings, we need to investigate the SLAC data at 9.3 GeV. Specifically we look at the natural components at the SDME. Assuming only one exchange, our form in Eq. (4) for the top vertex leads to

$$\rho_{00}^N = \frac{\beta_1^2}{N} \frac{-t}{m_V^2} \quad (15a)$$

$$\text{Re } \rho_{10}^N = \frac{\beta_1}{2N} \frac{\sqrt{-t}}{m_V} \left(1 + \beta_2 \frac{-t}{m_V^2} \right) \quad (15b)$$

$$\rho_{1-1}^N = \frac{\beta_1^2}{N} \frac{-t}{m_V^2} \quad (15c)$$

with $N = 1 - \beta_1^2 t / m_V^2 + \beta_2^2 t^2 / m_V^4$. The factorization hypothesis and the conservation of angular momentum implies the vanishing of these SDME in the forward direction. This fact is indeed observed in all the ρ^0 SDME but is inconsistent with the ρ_{1-1}^N elements for ω photoproduction as seen on Fig. 4. The expressions in Eqs (15) also tell us

that we should expect $\rho_{00}^N < \text{Re} \rho_{10}^N$ in the forward direction. Again this relation is satisfied for ρ^0 photoproduction but is clearly violated in ω photoproduction. The element ρ_{00}^N is significantly bigger in ω photoproduction compared to ρ^0 photoproduction, suggesting a larger single helicity flip for the isovector exchange. The deviation from zero in the elements $\text{Re} \rho_{10}^N$ and ρ_{1-1}^N for ρ^0 photoproduction suggests non-zero single and double helicity flip for the isoscalar exchanges. We associate these couplings to only the f_2 exchange and keep the Pomeron helicity conserving as often assumed. This latter hypothesis could be checked on ϕ photoproduction as we will discuss later. According to our discussion we impose $\beta_1^{\mathbb{P}} = \beta_2^{\mathbb{P}} = \beta_2^{a_2} = 0$. The remaining couplings $\beta_1^{a_2}, \beta_1^{f_2}$ and $\beta_2^{f_2}$ are fitted on the three ρ^0 natural exchange SDME and the ρ_{00}^N for ω photoproduction. We do not include the two other SMDE elements in ω photoproduction as they are inconsistent with our working hypothesis. The fit of the total cross sections discussed above and the fit of the SLAC SDME are combined in a single fit. There are 423 (total cross sections) plus 24 (SDME) data points in total for six parameters. The other model parameters (the b_R , the κ_R , the γ_V and the pion and eta exchange couplings) are kept fixed during the calculation. Note that we do not use the approximated expressions (15) but the full expression for the natural components of the SDME, cf. Eq. (B3). Our resulting $\chi^2/\text{d.o.f.}$ is 2.7 and the fitted parameters are

$$\beta_{\mathbb{P}}^{\gamma\gamma} = 0.188(1) \qquad \beta_1^{f_2} = 0.85(18) \qquad (16a)$$

$$\beta_{f_2}^{\gamma\gamma} = 0.152(2) \qquad \beta_2^{f_2} = -0.47(14) \qquad (16b)$$

$$\beta_{f_2}^{\gamma\gamma} = 0.041(2) \qquad \beta_1^{a_2} = 0.79(35) \qquad (16c)$$

Of course at each stage the photon-vector meson couplings are extracted from Eqs (11). The parameters of the natural exchanges needed for vector meson photoproduction are summarized in Table III.

TABLE III. Model parameters for the natural exchanges.

	\mathbb{P}	f_2	a_2
$\beta^{\gamma\omega}$	0.744(1)	0.677(7)	1.137(62)
$\beta^{\gamma\rho}$	2.523(4)	2.297(25)	0.335(18)
$\beta^{\gamma\phi}$	0.939(2)	0	0
b	4	0.5	0.5
β_1	0	0.85(18)	0.79(35)
β_2	0	-0.47(14)	0

IV. COMPARISON WITH DATA

As we discussed above the SDME elements for ρ^0 photoproduction are more consistent with our model for diffractive production than for ω photoproduction. Our model thus better describes these former data as can be seen in Fig. 4. The larger uncertainties in the ω model originate from the stronger dominance of the Regge exchanges, whose normalization are less constrained by the total cross sections. The Pomeron normalization is indeed more constrained and yields a smaller uncertainty in the ρ^0 model. We have also included the data at $E_\gamma = 4.7$ and 2.8 GeV from SLAC on Fig. 4. They compare reasonably well to our extrapolated model.

On Fig. 5, we present the comparison between the ω and ρ^0 models and the SLAC data at 9.3 GeV. There is a general agreement between the model and the data although some inconsistencies are pointed out. The elements in the bottom lines ρ_{1-1}^1 , $\text{Im} \rho_{10}^2$ and $\text{Im} \rho_{1-1}^2$ were not included in the fitting procedure but are very well described by our model. In particular, we note the dominance of the natural exchanges in ρ_{1-1}^1 and $\text{Im} \rho_{1-1}^2$ in the case of ρ^0 photoproduction with small deviation for the ω case, as expected from the stronger pion exchange. The main noticeable discrepancy arise in ρ_{11}^1 for ω photoproduction. Since the pseudoscalar exchanges are relatively smaller than the natural exchanges, we would expect $\rho_{11}^1 \sim \rho_{1-1}^0$. The data do not display this feature and thus our model doesn't describe well ρ_{11}^1 . The contribution from the pion exchange to ρ_{11}^1 is negative, cf. App. C, we would thus expect $\rho_{11}^1 < \rho_{1-1}^0$, which is featured in our ω model but not in the SLAC data. The sign of the element ρ_{11}^1 would be an important check for our model when the GlueX data will be available.

Although our model has been designed for $E_\gamma = 9$ GeV, we present on Fig. 6, the comparison between our model and the unpolarized SDME at lower energies. Given the significant uncertainties in all data sets presented, we conclude that our extrapolated model describes fairly well the lower energies data sets. It is worth noting also that the data from Ref. [24] at $E_\gamma = 8.9$ GeV, are consistent with our factorization hypothesis, *i.e.* $\rho_{1-1}^0 \sim 0$ in the forward direction. We conclude that the SLAC data may suffer from large statistical fluctuations. The forthcoming measurement by the

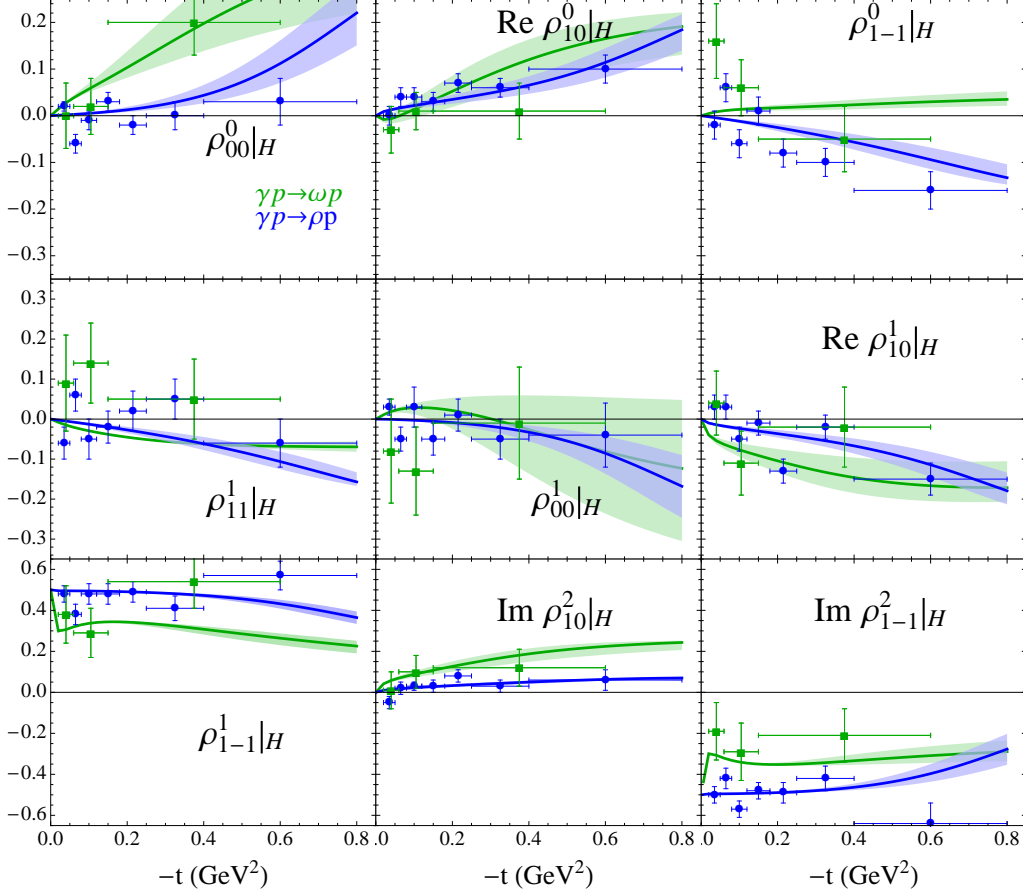


FIG. 5. Spin density matrix elements of ω and ρ^0 photoproduction at $E_\gamma = 9.3$ GeV. Data from Ref. [7]. The lines are our model.

GlueX collaboration could confirm the factorization of the vector meson production, *i.e.* $\rho^0_{1-1}(t) \sim |t|$ in the forward direction.

Our model simplifies for ϕ photoproduction. In this case we simply neglect the f_2 and a_2 Regge exchanges, as they are not expected to couple to $\gamma\phi$. The relevant exchange would be the f'_2 , the hidden strange partner of the f_2 exchange. However, its intercept, and therefore its overall strength, is smaller due its higher mass. We neglect this contribution and assume that the only relevant natural contribution is provided by the Pomeron. Since our Pomeron is purely helicity conserving, the SDME are very simple at high energy. The only non-zero component are $\rho^1_{1-1} = -\text{Im} \rho^2_{1-1} = 1/2$. This picture is consistent with the SLAC measurement at 9.3 GeV [7]. On Fig. 7, we compare our model to the data from the Omega photon collaboration [26]. Their data are taken in the energy range $E_\gamma = 20 - 40$ GeV. They are consistent with the SLAC data but have somewhat smaller uncertainties. We also extrapolated our model to $E_\gamma = 2.27$ GeV to compare with the data from the LEPS collaboration [25]. At lower energies, we observe deviation from pure helicity conservation. This is triggered by unnatural exchanges. Since the pion couples weakly to $\gamma\phi$, we included the η exchange in our model. Indeed the very small coupling $g_{\phi\gamma\eta}$, inferred from radiative decays cf. Table I, cannot solely explain the deviation from helicity conservation ($\rho^1_{1-1} = -\text{Im} \rho^2_{1-1} = 1/2$) at $E_\gamma = 2.27$ GeV. The inclusion of η exchange describes well the SDME from the LEPS collaboration. Although we should note that we needed to consider the η degenerate with the pion. The η pole being further from the scattering region, the factor $\alpha'\pi/\sin\pi\alpha_\eta(t) \sim 1/(m_\eta^2 - t)$ is not strong enough to trigger the depletion close to the forward direction in ρ^1_{1-1} and $\text{Im} \rho^2_{1-1}$. As we pointed out the Pomeron coupling $g_{\mathbb{P}}^{\gamma\phi}$ from the ϕ meson leptonic width and VMD is overestimated. The relative strength of the unnatural exchanges in the SDME are thus underestimated. We compensate this effect by choosing the η nucleon coupling $g_{\eta NN}^2/4\pi = 2$ are the higher end of its common value. Instead of estimating the various contribution theoretically, an alternative would be to determine directly from the data the ratio of the

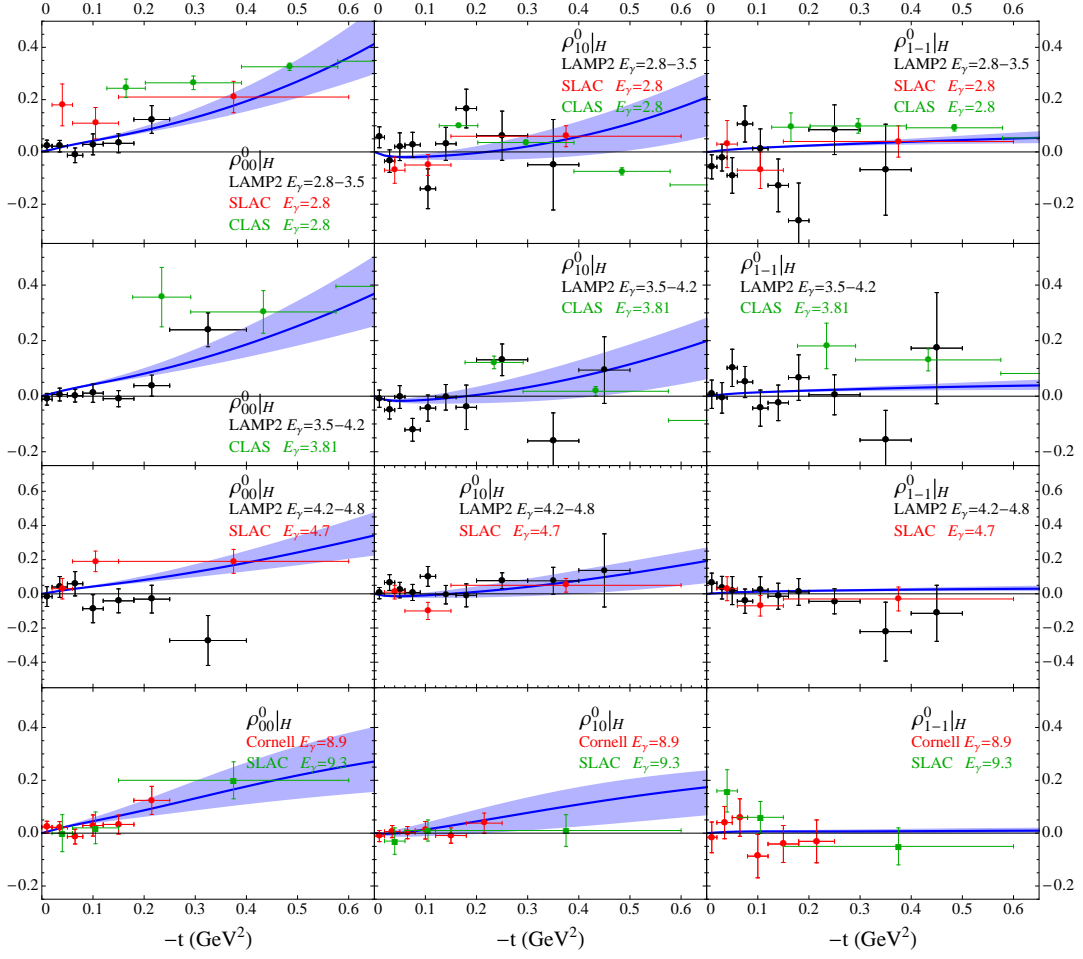


FIG. 6. Unpolarized spin density matrix elements of ω photoproduction. Data from Ref. [7] (SLAC), Ref. [22] (CLAS 2.8 GeV), Ref. [23] (LAMP2) and Ref. [24] (Cornell). The lines are our model.

unnatural versus natural component. Since the helicity conserving Pomeron and the pseudoscalar exchange have, respectively, only one coupling, ϕ meson SDME provide an indication of their ratio.

Our prediction for vector meson ω, ρ^0, ϕ photoproduction at GlueX is displayed on Fig. 8. We used $E_\gamma = 8.5$ GeV, the average beam energy with polarized beam. As already commented, the main bulk of the uncertainties in our model comes from the Regge exchanges. It is therefore not surprising that the uncertainties in the ϕ meson SDME are very small. The bending of the curves as $|t|$ increases in our ϕ model originate from the pseudoscalar exchanges. We haven't included an exponential falloff in their parametrization. Therefore their effects can be observed away from the forward direction where the natural exchanges are exponentially suppressed. That could be just an artifact of the model. If the ϕ SDME remain flat in a larger t range, one would just need to incorporate an exponential falloff in the η exchange. Our model will be soon available on the JPAC interactive website [27, 28]. It will be possible to vary the model parameters online and generate the SMDE for ρ^0, ω and ϕ photoproduction.

Our model has been designed to describe SDME. We mainly focused on the helicity structure at the photon-vector meson vertex. We can however compare our simple model to the differential cross sections. We first compare our model to high energy data on Fig. 9. At energies above 50 GeV, the Regge exchanges contribute for less than 1% of the differential cross section. The data gives therefore a very good indication of the validity of our Pomeron model. We observed that the overall normalization is in fairly good agreement with the data. Of course, our phenomenological intercept $\alpha_{\mathbb{P}}(0) = 0.08$ produces a slightly rise of the differential cross section in the forward direction. At very high energy, $E_\gamma > 1$ TeV, the data seems to display a slower growth, in agreement with the unitarity bound. These energies are however far from our region of interest. The t -dependence was approximated by a simply exponential falloff, which describes well the data in the range $0 < -t/m_V^2 < 1$. With the logarithmic scale, we observe a bending

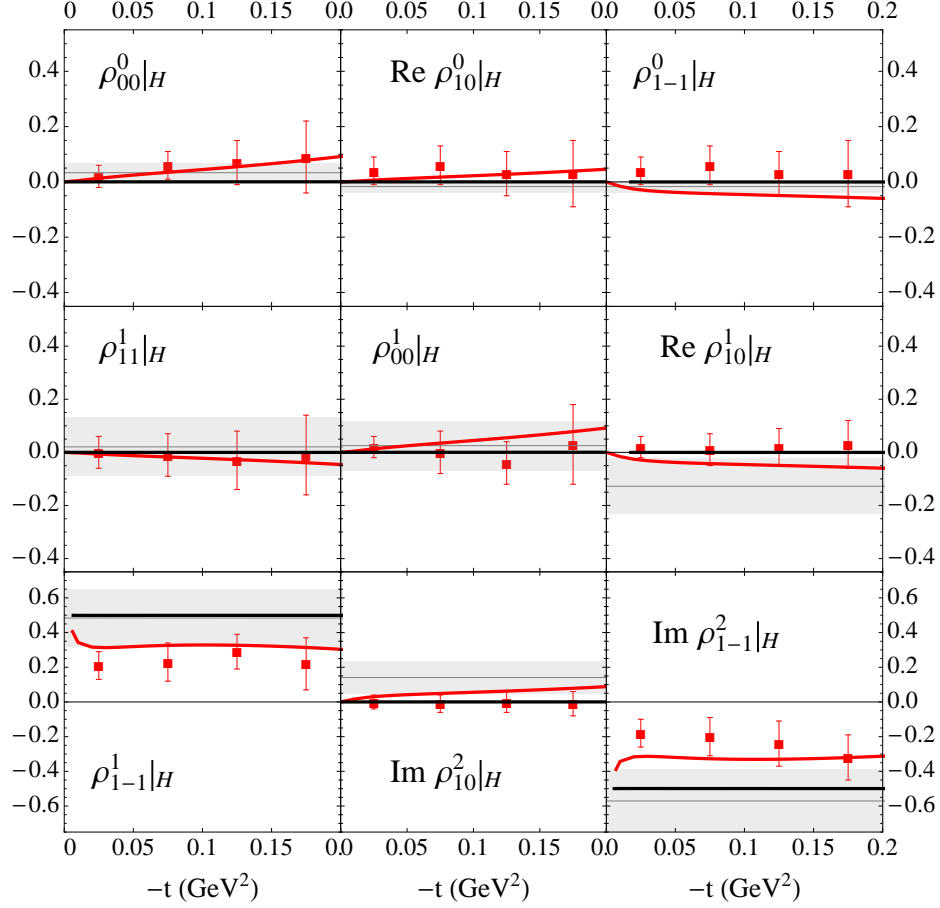


FIG. 7. Spin density matrix elements of ϕ photoproduction at $E_\gamma = 2.17 - 2.37$ GeV (red squared) from Ref. [25] and at $E_\gamma = 20 - 40$ GeV (gray band) from Ref. [26]. The lines are our model at $E_\gamma = 2.27$ (red) and $E_\gamma = 30$ GeV (black).

of the differential cross section that could be described by a form factor like in Eq. (12).

Unfortunately our model does not compare very well to the differential at 9.3 GeV, cf. Fig. 10. Although the ρ^0 and ω differential cross section are roughly in agreement with our model, the ϕ differential cross section is overestimated. We already explained that the leptonic width of the ϕ meson led to a Pomeron coupling to $\gamma\phi$ much stronger than the experimental value. It was already observed the original experimental publication [7]. It has been argued that the large ϕ mass need to be taken into account. The authors of Refs. [29, 30] corrected the differential by the ratio of the ϕ and photo momenta, $(k_\phi/k_\gamma)^2 \approx 0.87$ at $E_\gamma = 9.3$ GeV. This factor is nevertheless not small enough to reproduce the experimental normalization of the ϕ differential cross section.

V. CONCLUSION

We presented a model describing the SDME of light vector meson photoproduction. Our model includes a pion and a eta meson exchange, whose parameters are fixed. We incorporated the relevant natural exchanges, Pomeron, f_2 and a_2 exchanges. Their normalization were determined with on the total cross section using the VMD hypothesis. We paid special attention to the t dependence of the various exchanges. We proposed a flexible and intuitive ansatz for the t dependence of each natural exchange. The helicity structure of these exchanges are then inferred from the photoproduction of ω and ρ^0 at $E_\gamma = 9.3$ GeV at the SLAC facility. The joint inspection of these two reactions allowed us to assumed that the f_2 isoscalar exchange must have a small double helicity flip couplings, in addition to a single helicity flip coupling. The a_2 isovector exchange was consistent only only a single flip and no double helicity couplings.

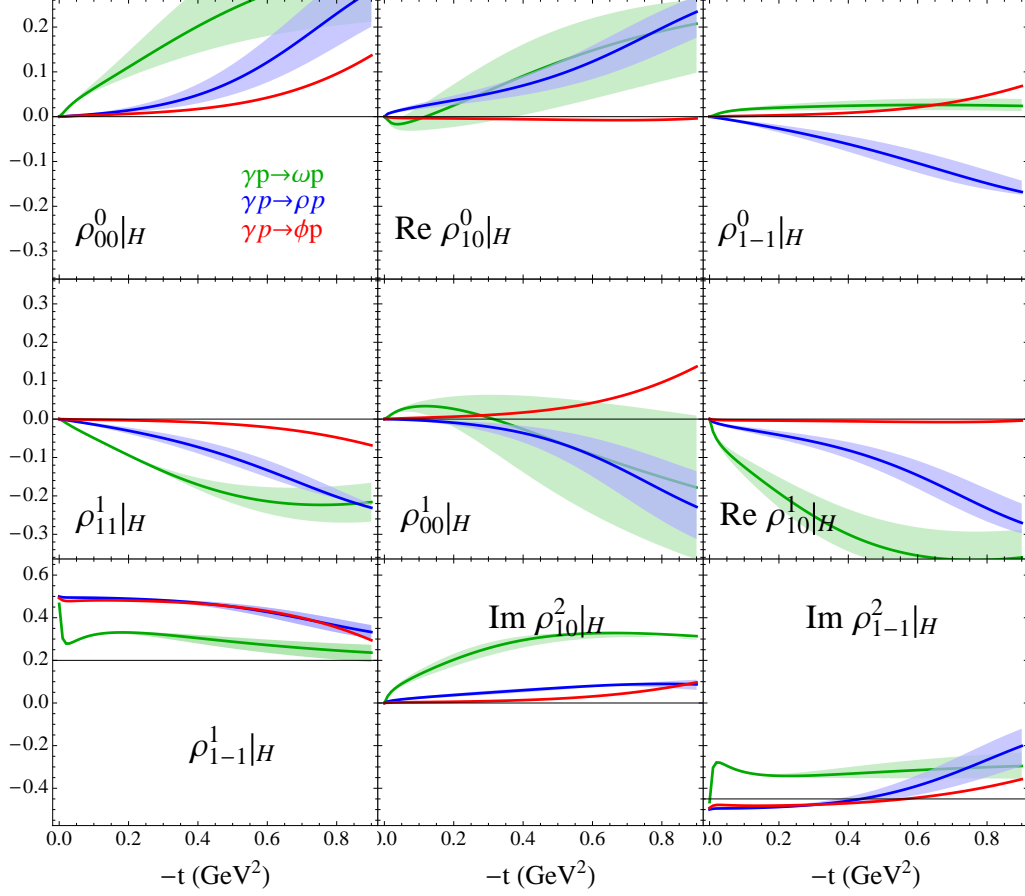


FIG. 8. Spin density matrix elements of ω , ρ^0 and ϕ photoproduction at $E_\gamma = 8.5$ GeV.

The model compared well to the nine SDME elements for each ρ^0 , ω and ϕ photoproduction in a wide energy range $E_\gamma \sim 3 - 9$ GeV. The model also compared well to the unpolarized data from various experiment in the same energy range. We made predictions for the future measurements of light meson photoproduction at GlueX. Our predictions and our model will be soon available online on the JPAC website [27, 28].

The differential cross section at very high energy, $E_\gamma > 50$ GeV is well reproduced by our Pomeron exchange. However the effect of the high energy approximation led to non negligible deviation from the data at $E_\gamma = 9.3$ GeV. These deviation appear only the differential cross section since they cancel in the ratio of SDME.

ACKNOWLEDGMENTS

We would like to thank C. Meyer for pointing out the future measurements by the GlueX collaboration and suggesting this work. This work was supported by BMBF, the U.S. Department of Energy under grants No. DE-AC05-06OR23177 and No. DE-FG02-87ER40365, PAPIIT-DGAPA (UNAM, Mexico) grant No. IA101717, CONACYT (Mexico) grant No. 251817, Research Foundation – Flanders (FWO), U.S. National Science Foundation under award numbers PHY-1507572, PHY-1415459 and PHY-1205019, and Ministerio de Economía y Competitividad (Spain) through grant No. FPA2016-77313-P.

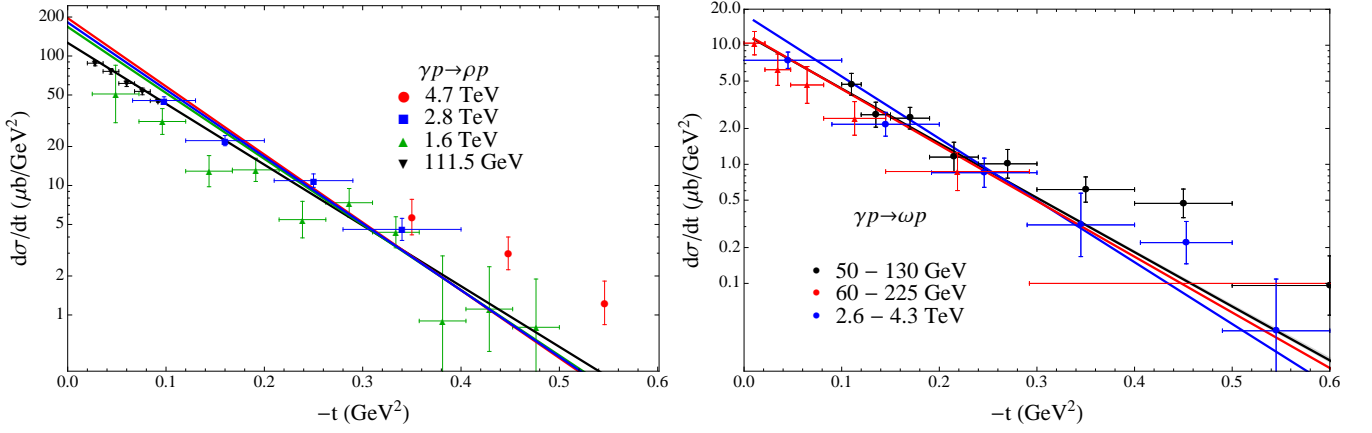


FIG. 9. $\gamma p \rightarrow \rho^0 p$ (left) and $\gamma p \rightarrow \omega p$ (right) differential cross sections at high energies. Data from Refs [1].

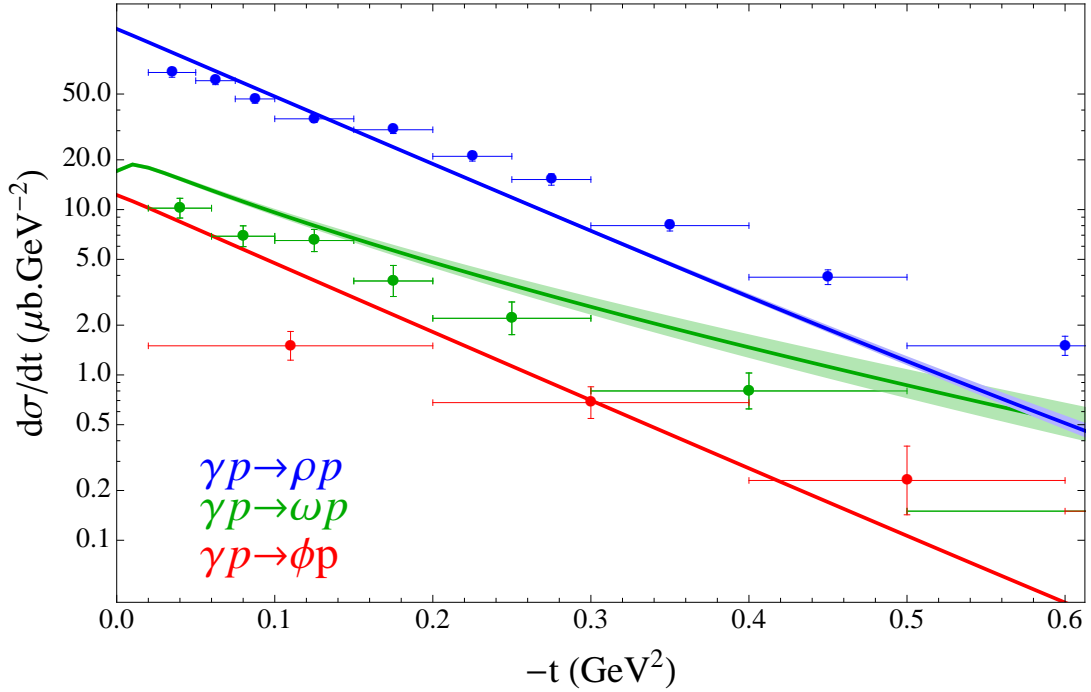


FIG. 10. $\gamma p \rightarrow (\rho^0, \omega, \phi)p$ differential cross section at 9.3 GeV. Data from Ref [7].

Appendix A: Frames

The properties of helicity amplitudes are best described in two popular frames: the s -channel and the t -channel frames. The s -channel corresponds to the center-of-mass of the reaction $\gamma p \rightarrow Vp$. The t -channel correspond to the center-of-mass of the reaction $\gamma \bar{V} \rightarrow p\bar{p}$. These channels are illustrated on Fig. 11.

The angular distribution of a vector meson is analyzed in his rest frame. In the rest frame of the vector meson, the beam, target and recoil form the reaction plane Oxz , the y -axis being defined as the cross product between the target and the recoil momenta. For the z axis, the two common choices are the opposite direction of the recoil (helicity frame) and the beam direction (Gottfried-Jackson frame).

The helicity amplitudes in these four frames are different. For instance the boost along the recoil momentum between the s -channel and the helicity frames rotates the helicities of the beam, target and recoil. It also transforms the helicity of the vector meson in the s -channel into into its spin projection along the direction opposite to the recoil in the helicity frame. The summation over beam, target and recoil helicities in the spin density matrix elements is

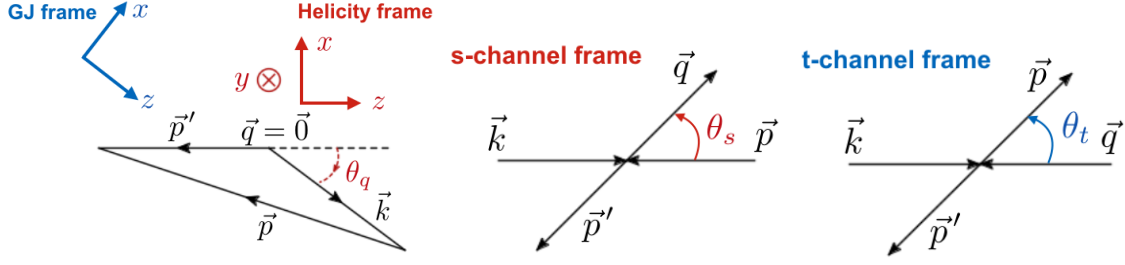


FIG. 11. Frame definition. See text for their relations.

not affected by these rotations. Hence the spin density matrix elements in the s —channel and helicity frames are equivalent.

Similarly the boost along the beam direction between the t -channel and the Gottfried-Jackson frames brings the helicity of the vector in the t -channel to its spin projection along the beam direction in the Gottfried-Jackson frame. The helicities of the other particles undergo a rotation which do not affect the spin density matrix elements as demonstrated in Ref [31].

Finally, from the spin density element in the Gottfried-Jackson frame, the spin density matrix elements in the helicity frame are obtained by a rotation of angle θ_q , the angle between the opposite direction of the recoil and the beam direction (cf Fig. 11)

$$\rho_{MM'}|_H = \sum_{\lambda_V, \lambda'_V} d_{M, \lambda_V}^1(\theta_q) \rho_{\lambda_V, \lambda'_V}|_{GJ} d_{M', \lambda'_V}^1(\theta_q) \quad (A1)$$

with $\cos \theta_q = (\beta - \cos \theta_s)/(\beta \cos \theta_s - 1)$ and $\beta = \lambda^{1/2}(s, m^2, m_V^2)/(s - m^2 + m_V^2)$. The leading s expression is simply $\cos \theta_q \rightarrow (m_V^2 + t)/(m_V^2 - t)$.

Appendix B: Spin Density Matrix Elements

The relation between SDME and helicity amplitudes are well-know [6]. For completeness we provide the expressions for the nine SDME accessible with a linearly polarized photon beam:

$$\rho_{00}^0 = \frac{1}{N} \sum_{\lambda, \lambda'} \mathcal{M}_{\lambda, \lambda'}^{1,0} \mathcal{M}_{\lambda, \lambda'}^{*1,0} \quad (\text{B1a})$$

$$\text{Re } \rho_{10}^0 = \frac{1}{2N} \text{Re} \sum_{\lambda, \lambda'} \left(\mathcal{M}_{\lambda, \lambda'}^{1,1} - \mathcal{M}_{\lambda, \lambda'}^{1,-1} \right) \mathcal{M}_{\lambda, \lambda'}^{*1,0} \quad (\text{B1b})$$

$$\rho_{1-1}^0 = \frac{1}{N} \text{Re} \sum_{\lambda, \lambda'} \mathcal{M}_{\lambda, \lambda'}^{1,1} \mathcal{M}_{\lambda, \lambda'}^{*1,-1} \quad (\text{B1c})$$

$$\rho_{11}^1 = \frac{1}{N} \text{Re} \sum_{\lambda, \lambda'} \mathcal{M}_{\lambda, \lambda'}^{-1,1} \mathcal{M}_{\lambda, \lambda'}^{*1,1} \quad (\text{B1d})$$

$$\rho_{00}^1 = \frac{1}{N} \text{Re} \sum_{\lambda, \lambda'} \mathcal{M}_{\lambda, \lambda'}^{-1,0} \mathcal{M}_{\lambda, \lambda'}^{*1,0} \quad (\text{B1e})$$

$$\rho_{1-1}^1 + \text{Im } \rho_{1-1}^2 = \frac{1}{N} \sum_{\lambda, \lambda'} \mathcal{M}_{\lambda, \lambda'}^{-1,1} \mathcal{M}_{\lambda, \lambda'}^{*1,-1} \quad (\text{B1f})$$

$$\rho_{1-1}^1 - \text{Im } \rho_{1-1}^2 = \frac{1}{N} \sum_{\lambda, \lambda'} \mathcal{M}_{\lambda, \lambda'}^{1,1} \mathcal{M}_{\lambda, \lambda'}^{*-1,-1} \quad (\text{B1g})$$

$$\text{Re } \rho_{10}^1 + \text{Im } \rho_{10}^2 = \frac{1}{N} \text{Re} \sum_{\lambda, \lambda'} \mathcal{M}_{\lambda, \lambda'}^{-1,1} \mathcal{M}_{\lambda, \lambda'}^{*1,0} \quad (\text{B1h})$$

$$\text{Re } \rho_{10}^1 - \text{Im } \rho_{10}^2 = \frac{1}{N} \text{Re} \sum_{\lambda, \lambda'} \mathcal{M}_{\lambda, \lambda'}^{1,1} \mathcal{M}_{\lambda, \lambda'}^{*-1,0} \quad (\text{B1i})$$

Of course the SDME and the helicity amplitude need to be define in the same frame, or in equivalent frames, as explained in the previous section. The (frame-independent) normalization is

$$N = \frac{1}{2} \sum_{\lambda_\gamma, \lambda_V, \lambda, \lambda'} |\mathcal{M}_{\lambda_\gamma, \lambda_V}^{\lambda, \lambda'}|^2. \quad (\text{B2})$$

The SDME in Eqs (B1) provide useful information concerning the helicity structure of the photon-vector meson vertex. For instance, the element ρ_{00}^0 and ρ_{1-1}^0 give indication of the magnitude of the single flip contribution and the interference between the non-flip and the double-flip amplitudes. Moreover, they can use use to separate the contribution from natural and unnatural exchanges. Indeed, at high energies, a exchange with positive naturality (N) or negative naturality (U), satisfies

$$\mathcal{M}_{-\lambda_\gamma, -\lambda_V}^N = \pm \mathcal{M}_{\lambda_\gamma, \lambda_V}^N. \quad (\text{B3})$$

We can then use six SDME to get information about the helicity structure of natural and unnatural components:

$$\begin{aligned}\rho_{00}^N &= \frac{1}{2} (\rho_{00}^0 \mp \rho_{00}^1) \\ &= \frac{1}{N} \sum_{\lambda, \lambda'} \mathcal{M}_{1,0}^N \mathcal{M}_{1,0}^{N*}\end{aligned}\quad (\text{B4a})$$

$$\begin{aligned}\text{Re } \rho_{10}^N &= \frac{1}{2} (\text{Re } \rho_{10}^0 \mp \text{Re } \rho_{10}^1) \\ &= \frac{1}{2N} \text{Re} \sum_{\lambda, \lambda'} \left(\mathcal{M}_{1,1}^N - \mathcal{M}_{1,-1}^N \right) \mathcal{M}_{1,0}^{N*}\end{aligned}\quad (\text{B4b})$$

$$\begin{aligned}\rho_{1-1}^N &= \frac{1}{2} (\rho_{1-1}^1 \pm \rho_{11}^1) \\ &= \frac{1}{N} \text{Re} \sum_{\lambda, \lambda'} \mathcal{M}_{1,1}^N \mathcal{M}_{1,-1}^{N*}\end{aligned}\quad (\text{B4c})$$

The hypothesis of helicity conservation at the photon vertex, *i.e.* $\mathcal{M}_{\lambda_\gamma, \lambda_V} \propto \delta_{\lambda_\gamma}^{\lambda_V}$ can easily check on the SDME. As can be readily checked with Eqs (B1), this hypothesis leads to vanish SDME except for $\text{Im } \rho_{11}^1$ and $\text{Im } \rho_{1-1}^2$.

Appendix C: High Energy Limit

At high energy, models for amplitude reaction simplifies and provide intuitive formulas easily test again data. In this section, we perform the high energy limit of standard interaction and keep the leading order in s , the total energy squared. Our goal is to derive the t -dependence arising from the factorization of Regge poles. We consider the reaction $\gamma(k, \lambda_\gamma) p(p, \lambda) \rightarrow V(q, \lambda_V) p(p', \lambda')$ in the center-of-mass frame (s -channel frame). Let m and m_V be the nucleon and vector meson masses. We choose the z axis along the beam momentum and the y axis perpendicular to the reaction plane, $\mathbf{y} = \hat{\mathbf{k}} \times \hat{\mathbf{q}}$.

Let us first focus on the pseudoscalar exchanges. According to the factorization theorem of Regge pole, the interaction is a product of a γVP vertex, a Regge factor and a PNN vertex. At the photon vertex we use

$$\mathcal{V}_{\lambda_\gamma \lambda_V} = ig_{VP\gamma} \varepsilon_{\alpha\beta\mu\nu} \epsilon^\alpha(\lambda_\gamma) \epsilon^{*\beta}(\lambda_V) k^\mu q^\nu. \quad (\text{C1})$$

In the center-of-mass, the angular dependence of this interaction is instructive

$$\mathcal{V}_{\lambda_\gamma \lambda_V} \propto \left(\cos \frac{\theta_s}{2} \right)^{|\lambda_\gamma + \lambda_V|} \left(\sin \frac{\theta_s}{2} \right)^{|\lambda_\gamma - \lambda_V|}, \quad (\text{C2})$$

with θ_s , the scattering angle in the s -channel frame. This factor, known as the half-angle factor, encodes all the t -dependence of the interaction. At large energies, the t -dependence of the half-angle factor becomes very intuitive,⁴ $\sin \theta_s/2 \rightarrow 2\sqrt{-t}/s$ and $\cos \theta_s/2 \rightarrow 1$. Keeping only the leading term in s of the interaction in Eq. (C3), we obtain

$$\mathcal{V}_{\lambda_\gamma \lambda_V} \rightarrow -g_{VP\gamma} \lambda_\gamma \frac{m_V^2}{2} \left[\delta_{\lambda_\gamma}^{\lambda_V} - \sqrt{2} \lambda_\gamma \frac{\sqrt{-t}}{m_V} \delta_0^{\lambda_V} + \frac{-t}{m_V^2} \delta_{-\lambda_\gamma}^{\lambda_V} \right]. \quad (\text{C3})$$

This example illustrates a general statement: each helicity flip “costs” a factor $\sqrt{-t}/m_V$. The mass scale associated to the factor $\sqrt{-t}$ can only be the only scale at this vertex, m_V . For completeness, we derive the decay width from the interaction (C3):

$$\Gamma(V \rightarrow \gamma P) = \frac{g_{VP\gamma}^2}{96\pi} \left(\frac{m_V^2 - m_P^2}{m_V} \right)^3 \quad (\text{C4})$$

We will use Eq. (C4) to extract the couplings from the decay widths.

⁴ In the following we will denote by an arrow the leading term in s

The considerations observed at the photon vertex applies at the nucleon vertex. For an unnatural spin zero exchange there is only one possible structure at the nucleon vertex:

$$g_{PNN}\bar{u}(p', \lambda)\gamma_5 u(p, \lambda) \rightarrow g_{PNN}\sqrt{-t}\delta_{-\lambda'}. \quad (C5)$$

There is one unit of helicity flip associated with the factor $\sqrt{-t}$. In this case the scale factor, the nucleon mass, is implicitly removed by our spinor normalization $\bar{u}(p, \lambda)u(p, \lambda) = 2m$.

The Regge factor is normalized to reduce to the pion propagator around the pion pole:

$$\pi\alpha' \frac{1 + e^{-i\pi\alpha(t)}}{2 \sin \pi\alpha_\pi(t)} \sim \frac{1}{m_\pi^2 - t}. \quad (C6)$$

Finally collecting all the pieces and summing over pion and eta exchanges, we arrive to the amplitude in Eq. (C7). Given the mass difference between the pion and the eta meson, it might be surprising to use the same Regge trajectory for both exchanges. However the eta contributes significantly only in the photoproduction of ϕ meson. As we see in Sec. IV, the VMD hypothesis overestimates the contribution of the Pomeron exchange in ϕ production. Using the pion Regge trajectory enhance the eta contribution and partly compensates this effect when computing the SDME.

It is instructive to derive the SDME for only a pion exchange in both GJ and helicity frames. The SDME induced by a pion exchange takes a simple form in the GJ frame, *i.e.* all SDME are zero except for $\rho_{1-1}^1 = -\text{Im}\rho_{1-1}^2 = -\frac{1}{2}$. This is of course expected since the pion in its rest frame only have the spin projection zero. We can get easily get the SDME for a pion exchange in the helicity frame from the rotation in Eq. (A1):

$$\rho_{00}^0 = \rho_{00}^1 = \frac{-2t/m_V^2}{(1 - t/m_V^2)^2} \quad (C7a)$$

$$\rho_{1-1}^0 = -\rho_{11}^1 = \frac{-t/m_V^2}{(1 - t/m_V^2)^2} \quad (C7b)$$

$$\text{Re}\rho_{10}^0 = \text{Re}\rho_{10}^1 = \frac{-1}{\sqrt{2}} \frac{\sqrt{-t}}{m_V} \frac{1 + t/m_V^2}{(1 - t/m_V^2)^2} \quad (C7c)$$

$$\rho_{11}^0 = -\frac{1}{2} \frac{1 + t/m_V^2}{(1 - t/m_V^2)^2} \quad (C7d)$$

$$\text{Im}\rho_{1-1}^2 = -\frac{1}{2} \frac{1 - t/m_V^2}{(1 - t/m_V^2)^2} \quad (C7e)$$

$$\text{Im}\rho_{10}^2 = \frac{-1}{\sqrt{2}} \frac{\sqrt{-t}}{m_V} \frac{1}{(1 - t/m_V^2)^2} \quad (C7f)$$

In the case of a single exchange, the SDME depends only on the details on the photon vertex and the only scale arising is the mass of the vector meson.

The two guiding rules, the factorization of Regge poles and the factor of $\sqrt{-t}$ for each unit of helicity flip, equally apply to natural exchanges. We can then postulate the general form in Eq. (3). Since the use of effective Lagrangian is very popular, it is instructive to compare our model in Eq. (3) to these types of interaction.

Let us start by the standard interaction for a Pomeron exchange [20?]

$$\mathcal{M}_{\lambda_\gamma, \lambda_V}^{\mathbb{P}}(s, t) = \epsilon_\nu^*(q, \lambda_V) [k^\mu \epsilon^\nu(k, \lambda_\gamma) - k^\nu \epsilon^\mu(k, \lambda_\gamma)] \bar{u}(p', \lambda') \gamma_\mu u(p, \lambda) \quad (C8)$$

At leading order in s , we have $k^\mu \rightarrow n_+^\mu$ and

$$\bar{u}(p', \lambda') \gamma^\mu u(p, \lambda) \rightarrow \sqrt{s} \delta_{\lambda'}^{\lambda} n_-^\mu \quad (C9)$$

with $n_\pm^\mu = (1, 0, 0, \pm 1)$. Then only the first term in the bracket in Eq. (C8) survives. From the result

$$\epsilon^*(q, \lambda_V) \cdot \epsilon(k, \lambda_\gamma) \rightarrow -\lambda_\gamma^2 \delta_{\lambda_\gamma}^{\lambda_V} + \delta_0^{\lambda_V} \frac{\lambda_\gamma}{\sqrt{2}} \frac{\sqrt{-t}}{m_V}, \quad (C10)$$

we conclude that this model for the Pomeron implicitly includes a single helicity flip structure and is not therefore purely helicity conserving. A more flexible model can be obtained with more general interaction. In order to determine

all the possible structures, let us first observe that in a factorizable model, top and bottom vertices are linked by a propagator, transverse to the momentum transferred. The propagator removes the x component since $(q - k)^\mu \rightarrow (0, \sqrt{-t}, 0, 0)$ at leading order in s . Secondly, the general structures at the nucleon vertex are easily obtained. In addition to Eq. (C9), we can have a nucleon helicity flip interaction

$$\bar{u}(p', \lambda') (2p^\mu - \gamma^\mu) u(p, \lambda) \rightarrow 2\lambda\sqrt{-t}\delta_{-\lambda}^{\lambda'} n_-^\mu. \quad (\text{C11})$$

Note that any p' momentum can be substituted by p since the difference is orthogonal to the propagator. At the photon vertex, the only tensorial structure that connects to the nucleon vertex and survives at the leading s order are $k^\mu \rightarrow n_+^\mu$ and $\epsilon^*(q, \lambda_V) \rightarrow (1 - \lambda_V^2)(q/m_V)n_+^\mu$. We can then form a single helicity flip couplings at the photon vertex with the interaction

$$\epsilon^{\mu*}(q, \lambda_V) q \cdot \epsilon(k, \lambda_\gamma) \rightarrow \frac{1}{2} \frac{\lambda_\gamma}{\sqrt{2}} \frac{\sqrt{-t}}{m_V} \delta_0^{\lambda_V} n_+^\mu. \quad (\text{C12})$$

Since the maximum helicity difference between a photon and a vector meson in their center of mass is two, a tensor exchanges should involve all possible relevant structures at the photon vertex. We indeed find that a double flip structure can arise with the interaction with a photon, a vector and a tensor [32]:

$$\epsilon^*(q, \lambda_V) \cdot k \epsilon(k, \lambda_\gamma) \cdot q \rightarrow \lambda_\gamma \lambda_V \frac{t}{2}. \quad (\text{C13})$$

In addition to Eq. (C10), the general structure with a photon, a vector and a tensor [32] also includes the non-flip interaction in Eq. (C10) and the single flip interaction in Eq. (C11). At the leading order in s , we summarize all these interactions with the intuitive vertex in Eq. (4).

-
- [1] H. Al Ghouli *et al.* (GlueX), *Proceedings, 16th International Conference on Hadron Spectroscopy (Hadron 2015): Newport News, Virginia, USA, September 13-18, 2015*, AIP Conf.Proc. **1735**, 020001 (2016), arXiv:1512.03699 [nucl-ex].
 - [2] M. Battaglieri *et al.* (CLAS), “Jlab approved experiment e12-11-005,” (2011), https://www.jlab.org/exp_prog/proposals/11/PR12-11-005.pdf.
 - [3] H. Al Ghouli *et al.* (GlueX), Phys.Rev. **C95**, 042201 (2017), arXiv:1701.08123 [nucl-ex].
 - [4] R. L. Anderson, D. Gustavson, J. R. Johnson, I. Overman, D. Ritson, B. H. Wiik, and D. Worcester, Phys.Rev. **D4**, 1937 (1971).
 - [5] V. Mathieu, G. Fox, and A. P. Szczepaniak, Phys.Rev. **D92**, 074013 (2015), arXiv:1505.02321 [hep-ph].
 - [6] K. Schilling, P. Seyboth, and G. E. Wolf, Nucl. Phys. **B15**, 397 (1970), [Erratum: Nucl. Phys.B18,332(1970)].
 - [7] J. Ballam *et al.*, Phys. Rev. **D7**, 3150 (1973).
 - [8] W. Drechsler, Phys. Lett. **23**, 272 (1966).
 - [9] K. Schilling and F. Storim, Nucl. Phys. **B7**, 559 (1968).
 - [10] J. Daboul, Nucl. Phys. **B7**, 651 (1968).
 - [11] E. Gotsman, P. D. Mannheim, and U. Maor, Phys. Rev. **186**, 1703 (1969).
 - [12] J. P. Ader and M. Capdeville, Nucl. Phys. **B17**, 127 (1970).
 - [13] I. S. Barker, E. Gabathuler, and J. K. Storrow, Nucl. Phys. **B78**, 515 (1974).
 - [14] A. Sibirtsev, K. Tsushima, and S. Krewald, Phys. Rev. **C67**, 055201 (2003), arXiv:nucl-th/0301015 [nucl-th].
 - [15] B.-G. Yu and K.-J. Kong, (2017), arXiv:1710.04511 [hep-ph].
 - [16] P. D. B. Collins, *An Introduction to Regge Theory and High-Energy Physics*, Cambridge Monographs on Mathematical Physics (Cambridge Univ. Press, Cambridge, UK, 2009).
 - [17] M. Gell-Mann, D. Sharp, and W. G. Wagner, Phys. Rev. Lett. **8**, 261 (1962).
 - [18] C. Patrignani *et al.* (Particle Data Group), Chin. Phys. **C40**, 100001 (2016).
 - [19] A. Donnachie and P. V. Landshoff, Phys. Lett. **B348**, 213 (1995), arXiv:hep-ph/9411368 [hep-ph].
 - [20] Y.-s. Oh, A. I. Titov, and T. S. H. Lee, Phys. Rev. **C63**, 025201 (2001), arXiv:nucl-th/0006057 [nucl-th].
 - [21] A. C. Irving and R. P. Worden, Phys.Rept. **34**, 117 (1977).
 - [22] M. Williams *et al.* (CLAS), Phys. Rev. **C80**, 065208 (2009), arXiv:0908.2910 [nucl-ex].
 - [23] D. P. Barber *et al.* (LAMP2 Group), Z. Phys. **C26**, 343 (1984).
 - [24] J. Abramson, D. E. Andrews, J. R. Harvey, F. Lobkowicz, E. N. May, C. A. Nelson, Jr., M. Singer, E. H. Thorndike, and M. E. Nordberg, Jr., Phys. Rev. Lett. **36**, 1428 (1976).
 - [25] W. C. Chang *et al.* (LEPS), Phys. Rev. **C82**, 015205 (2010), arXiv:1006.4197 [nucl-ex].
 - [26] M. Atkinson *et al.* (Omega Photon), Z. Phys. **C27**, 233 (1985).
 - [27] JPAC Collaboration, “JPAC Website,” <http://www.indiana.edu/~jpac/>.
 - [28] V. Mathieu, *Proceedings, 16th International Conference on Hadron Spectroscopy (Hadron 2015): Newport News, Virginia, USA, September 13-18, 2015*, AIP Conf.Proc. **1735**, 070004 (2016), <http://www.indiana.edu/~jpac/>, arXiv:1601.01751 [hep-ph].

- [29] H. J. Behrend, J. Bodenkamp, W. P. Hesse, W. A. McNeely, Jr., T. Miyachi, D. C. Fries, P. Heine, H. Hirschmann, A. Markou, and E. Seitz, Nucl. Phys. B144, 22 (1978).
- [30] D. P. Barber *et al.*, Z. Phys. C12, 1 (1982).
- [31] K. Gottfried and J. D. Jackson, Nuovo Cim. 33, 309 (1964).
- [32] N. Levy, P. Singer, and S. Toaff, Phys. Rev. D13, 2662 (1976).